An Analysis of User Mobility in Cellular Networks

Shamma Nikhat
Dept. of Electrical & Comp. Eng.
Concordia University
Montreal, Canada
r_nikhat@encs.concordia.ca

Mustafa Mehmet-Ali
Dept. of Electrical & Comp. Eng.
Concordia University
Montreal, Canada
mustafa@ece.concordia.ca

ABSTRACT

User mobility impacts the performance of cellular networks. However, there is a lack of results on this problem because of the difficulty of the analysis. The existing results are limited to handover rate and mean path length that a user is associated with the same base station. In this paper, we derive the probability distribution function of the path length that a user will be associated with the same base station. It is assumed that the user travels along a straight path and it is associated to the nearest base station. We make the stochastic geometry assumption that the base stations are distributed over the area according to a Poisson point process. We provide simulation results as further evidence that the analysis is correct. The results of this paper may be useful in the design of cellular networks.

KEYWORDS

User mobility; cellular networks; handover; path length distribution

ACM Reference format:

Shamma Nikhat and Mustafa Mehmet-Ali. 2018. An Analysis of User Mobility in Cellular Networks. In Proc. of 16th ACM Int'l Symposium on Mobility Management and Wireless Access, Montréal, Québec, Canada, October 28–November 2, 2018 (MobiWac'18), 8 pages. https://doi.org/10.1145/3265863.3265878

1 INTRODUCTION

The impact of mobility on the performance of the cellular networks is important, since most of the time users receiving service are mobile. As the user moves from one cell to the neighboring cell, then the user has to be served by the new cell and this requires handover. Handover increases the network load as it increases signaling overhead. The rapid growth of the demand for wireless communications has led to the need of increasing capacity of wireless networks. Since the amount of available spectrum is limited, this has resulted in shrinking of the cell sizes to increase spectrum reuse and consequently the wireless network capacity. However, handover rate, mean number of handovers per unit time, increases with decreasing cell size and with higher mobility [1].

Despite of the significance of user mobility, there is a lack of results on this problem, because of difficulty of the analysis. Initially, queueing networks was used to model mobility in cellular networks. In those models, each cell would be modeled as a queue and handoff would be modeled as transfer of a customer from one queue to another [2, 3]. However, these results fail to capture geometric pattern of the base stations in the plane. Recently, results from stochastic geometry has been applied in the studying of wireless networks. This technique assumes that the base stations are distributed according to a Poisson Point Process (PPP) over the plane [4]. This technique has also been applied to the study of the user mobility in the cellular networks. The main performance measures of interest have been handover rate and mean sojourn time. Sojourn time refers to the amount of time that a user spends in a cell. In [5], it is assumed that a user follows a variation of the random waypoint mobility (RWP) model. In RWP, a user travels in a certain direction for a random path length at a given speed, before changing the direction and speed randomly. In [5], they determine mean handover rate and mean sojourn time for single tier cellular networks. In [6], user mobility has been studied in multiple tiers of networks. They determine handoff rate for both horizontal and vertical handoffs, which refer to handoffs within a tier and across the tiers respectively for arbitrary user trajectories. In [7], they determine the mean sojourn time for a user moving at a constant speed along a randomly placed straight line in a cell that has the shape of convex polygon.

In this work, we assume that the user is moving along a straight path. Under the stochastic geometry assumption we determine probability distribution of path length without handover. This result corresponds to the distribution of the sojourn time for a user moving at a constant speed. We confirm

MobiWac'18, October 28–November 2, 2018, Montreal, QC, Canada

ACM ISBN 978-1-4503-5962-7/18/10...15.00
https://doi.org/10.1145/3265863.3265878

the correctness of the analysis through simulations. We think that as the network becomes more dense and multi-tier, more information than the handover rate will be needed to determine the performance of the system.

The remainder of the paper is organized as follows: Section 2. describes the system model, Section 3. derives conditional probability of no handover and Section 4. determines probability distribution of path length without handover. Finally, Section 5. presents the conclusions of the paper.

2 SYSTEM MODEL

Next, we describe the system model under consideration. We assume that the user moves along a straight line in small fixed size steps of d. We assume that the base stations are distributed in the plane according to a PPP with parameter λ stations/m^2. Let S_B denote the area of the region B in the plane, then probability of having k base stations in this region is given by,

$$P_k = \frac{e^{-\lambda S_B}(\lambda S_B)^k}{k!}, \quad k=0,1,2,... \tag{1}$$

We assume that the user will be served by the nearest base station, which will be referred to as the tagged base station.

We let A_i denote user location in the plane at the end of i'th step $i = 1,2, \ldots$ with initial user location being A_1. We let C denote the tagged base station when the user is at location A_1. We assume that when the user is at location A_i the tagged base station is still C. From Fig.1, this means that there are no base stations located within the circle centered at A_i that goes through C. Let us consider movement of the user from point A_i to A_{i+1} as shown in Fig. 1. The user to remain associated with the tagged base station C when it moves from A_i to A_{i+1}, then there should not be any stations located in the circle centered at A_{i+1} that goes through point C. We already know that there are no any base stations within the overlap area of these two circles. From Fig. 1, the user will remain associated with the tagged base station C at A_{i+1} if there are no base stations located within the non-overlapping area of the circle A_{i+1} with the circle A_i. As shown in Fig.1, let $S_{A_i \cap A_{i+1}}$ denote the area of the intersection of the circles centered at A_i and A_{i+1} respectively and $S_{A_{i+1}-(A_i \cap A_{i+1})}$ denote the nonoverlapping area of the circle centered at A_{i+1} with that centered A_i respectively. As a result probability of no handover as the user moves from point A_i to A_{i+1} will be given by,

$$\mathrm{P_r}(\text{no handover} \mid \text{tagged base station is } C) = \mathrm{P_r}\left(\text{no base station in } S_{A_{i+1}-(A_i \cap A_{i+1})}\right) \tag{2}$$

Substituting from equation (1),

$$\mathrm{P_r}(\text{no handover} \mid \text{tagged base station is } C) = exp(-\lambda S_{A_{i+1}-(A_i \cap A_{i+1})}) \tag{3}$$

In the next section, we will first determine the above conditional probability and in the section following that we will determine probability of the path length without handover.

In the following, we will let XY denote the line segment between the points X and Y and the length of this line segment as $|XY|$.

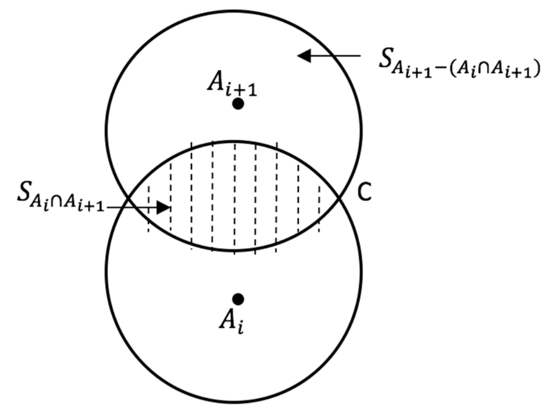

Figure 1: Intersection of the circles centered at A_i and A_{i+1} with tagged base station located at C.

3 DERIVATION OF THE PROBABILITY OF NO HANDOVER FOR SINGLE STEP USER MOVEMENT

Next, we will derive conditional probability that there is no handover as the user moves from location A_i to A_{i+1}given the location of the tagged base station C. In Fig. 1, we will assume that there is a Cartesian coordinate system located at point A_i with the straight line A_iA_{i+1} forming the y-axis. We will let (x_i, y_i) denote the Cartesian coordinates of C in this coordinate system.

Letting r_i denote the distance of C from A_i, then $r_i = |A_iC|$. Let r_{i+1} denote the distance of the user when it is located at A_{i+1} from the tagged base station C, $r_{i+1} = |A_{i+1}C|$. Then depending on the quadrant that the tagged base station is located there are four cases to be considered. Since the user is moving along the y-axis, the probability of no handover will be same for the positions of tagged base station C which are symmetric wrt y-axis. Thus we only need to analyze what happens when the tagged base station is in the first and fourth quadrants and multiply the resulting probability by two. In the case that the tagged base station is located in the first quadrant, there are two subcases depending on whether the step size is greater or smaller than the y-coordinate of the tagged base station. As a result, there are three cases to be considered depending on the location of the tagged base station C in quadrants I and IV.

Next, we will determine conditional probability of no handover for each of the cases by determining nonoverlapping area of the two circles for each of these cases. Since the user moves at steps of size d, then $d = |A_iA_{i+1}|$.

Case (i) : Tagged base station is in quadrant I and $y_i < d$.

This case has been shown in Fig. 2. Let θ_i, θ_{i+1} denote the angle between lines $A_iC, A_{i+1}C$ and the horizontal axis respectively. Similarly, let φ_i, φ_{i+1} denote the angle between lines $A_iC, A_{i+1}C$ and the vertical axis respectively.

$$\theta_i = \frac{\pi}{2} - \varphi_i \ , \qquad \theta_{i+1} = \frac{\pi}{2} - \varphi_{i+1} \tag{4}$$

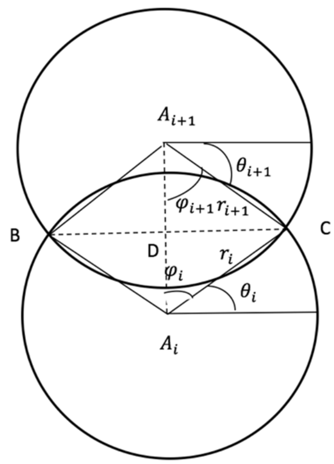

Figure 2: The network diagram when C is located in the first quadrant and $y_i < d$.

In Fig. 2, we let D denote the intersection of the lines A_iA_{i+1} and BC. As a result, we have,

$$|A_iD| = r_i sin\theta_i \ , \qquad |A_{i+1}D| = d - r_i sin\theta_i,$$

$$|CD| = |BD| = r_i cos\theta_i \tag{5}$$

$$r_{i+1} = \sqrt{|A_{i+1}D|^2 + |CD|^2}$$

Substituting in the above from (5),

$$r_{i+1} = \sqrt{(d - r_i sin\theta_i)^2 + r_i^2 cos^2\theta_i} \tag{6}$$

In Fig. 1, from the right triangle $\Delta A_{i+1}DC$,

$$\varphi_{i+1} = cos^{-1}\frac{|A_{i+1}D|}{|A_{i+1}C|} = cos^{-1}\frac{d - r_i sin\theta_i}{r_{i+1}} \tag{7}$$

where the second equation above follows from (5). From equation (4), θ_{i+1} is given by,

$$\theta_{i+1} = \frac{\pi}{2} - cos^{-1}\frac{d - r_{i+1} sin\theta_{i+1}}{r_{i+1}} \tag{8}$$

As shown in Fig. 3, let us define ∇A_iBC as the smaller of the sectors of the circle centered at A_i and the arc $\breve{BC}$. Similarly in Fig. 4, defining $\nabla A_{i+1}BC$ as the smaller of the sectors of the circle centered at A_{i+1} and the arc $\breve{BC}$. Next, let $S_{\nabla A_iBC}$, $S_{\nabla A_{i+1}BC}$ denote the areas of the circular sectors ∇A_iBC, $\nabla A_{i+1}BC$ respectively, then, from Fig. 2,

$$S_{\nabla A_iBC} = \varphi_i r_i^2 = r_i^2\left(\frac{\pi}{2} - \theta_i\right) \tag{9}$$

where the second equation follows from (4).

$$S_{\nabla A_{i+1}BC} = \varphi_{i+1} r_{i+1}^2 = r_{i+1}^2 cos^{-1}\frac{d - r_i sin\theta_i}{r_{i+1}} \tag{10}$$

where the second equation in the above follows from (5).

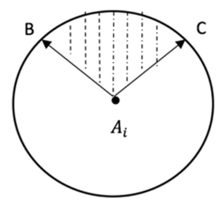

Figure 3: ∇A_iBC is the smaller of the sectors of the circle centered at A_i.

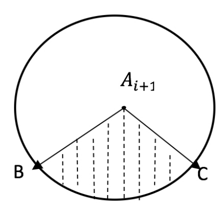

Figure 4: $\nabla A_{i+1}BC$ is the smaller of the sectors of the circle centered at A_{i+1}.

Next let $S_{\Delta A_iBC}, S_{\Delta A_{i+1}BC}$, denote the areas of the triangles ΔA_iBC, and $\Delta A_{i+1}BC$ as shown in Fig.s 5 and 6 respectively. Then from Fig. 2,

$$S_{\Delta A_iBC} = |A_iD| * |CD| = \frac{1}{2} r_i^2 sin2\theta_i \tag{11}$$

$$S_{\Delta A_{i+1}BC} = |A_{i+1}D| * |CD| = (d - r_i sin\theta_i) r_i cos\theta_i \tag{12}$$

where the second equations in the above follow from substitution from (5).

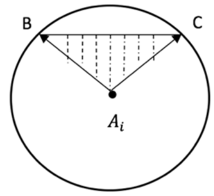

Figure 5: Triangle $\Delta A_i BC$

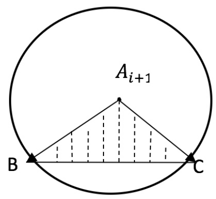

Figure 6. Triangle $\Delta A_{i+1} BC$

Next let $S_{A_{i+1}}$denote the area of the circle centered at A_{i+1} with radius r_{i+1},

$$S_{A_{i+1}} = \pi r_{i+1}^2 \tag{13}$$

Then, from Fig. 2, the area of the intersection of the circles centered at $A_i$and A_{i+1} respectively is given by,

$$S_{A_i \cap A_{i+1}} = S_{\nabla A_{i+1}BC} - S_{\Delta A_{i+1}BC} + S_{\nabla A_iBC} - S_{\Delta A_iBC} \tag{14}$$

The area of the circle at A_{i+1} that does not overlap with circle A_i,

$$S_{A_{i+1}-(A_i \cap A_{i+1})} = S_{A_{i+1}} - S_{A_i \cap A_{i+1}} \tag{15}$$

Substituting in the above from (9-13), then,

$$S_{A_{i+1}-A_i \cap A_{i+1}} = \pi r_{i+1}^2 - [{r_{i+1}}^2 cos^{-1}\frac{d - r_i sin\theta_i}{r_{i+1}} - (d - r_i sin\theta_i) r_i cos\theta_i + {r_{i+1}}^2 \left(\frac{\pi}{2} - \theta_i\right) - \frac{1}{2}{r_i}^2 sin2\theta_i]$$
(16)

Next substituting equation (16) in (3) gives us conditional probability of no handover as the user moves from point $A_i$to A_{i+1} for this case,

$$P_r(\text{no handover } | r_i \text{ and } \theta_i) = exp\left\{-\lambda\left[\pi r_{i+1}^2 - [{r_{i+1}}^2 cos^{-1}\frac{d - r_i sin\theta_i}{r_{i+1}} - (d - r_i sin\theta_i) r_i cos\theta_i + {r_{i+1}}^2\left(\frac{\pi}{2} - \theta_i\right) - \frac{1}{2}{r_i}^2 sin2\theta_i]\right]\right\} \tag{17}$$

We note that in the above (r_i, θ_i) gives the location of the tagged base station *C*.

Case (ii) : Tagged base station is in quadrant *I* and $y_i > d$.

This case is shown in Fig. 7 and the derivation of probability of no handover is similar to the previous case, therefore, we will only explain the differences and otherwise present the results.

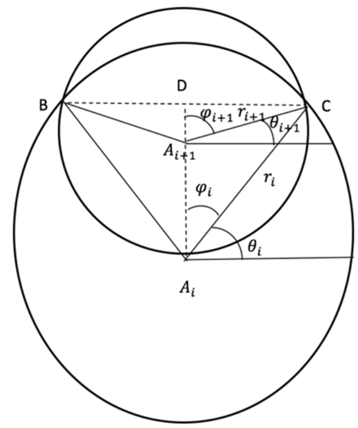

Figure 7: The network diagram when *C* is located in the first quadrant and $y_i > d$.

Equation (4) continues to hold for this case. In Fig. 7, we let *D* denote the extension of the line A_iA_{i+1} that intersects with *BC*. Then, we have,

$$|A_iD| = r_i sin\theta_i, \qquad |A_{i+1}D| = r_i sin\theta_i - d,$$
$$|CD| = |BD| = r_i cos\theta_i \tag{18}$$

As may be seen, $|A_{i+1}D|$ differs from the previous case. Next, we give the equations corresponding to (6-12) for this case,

$$r_{i+1} = \sqrt{(r_i sin\theta_i - d)^2 + {r_i}^2 cos^2\theta_i} \tag{19}$$

$$\varphi_{i+1} = cos^{-1}\frac{|A_{i+1}D|}{|A_{i+1}C|} = cos^{-1}\frac{r_i sin\theta_i - d}{r_{i+1}} \tag{20}$$

$$\theta_{i+1} = \frac{\pi}{2} - \varphi_{i+1} = \frac{\pi}{2} - cos^{-1}\frac{r_i sin\theta_i - d}{r_{i+1}} \tag{21}$$

$$S_{\nabla A_iBC} = \varphi_i {r_i}^2 = {r_i}^2\left(\frac{\pi}{2} - \theta_i\right) \tag{22}$$

$$S_{\nabla A_{i+1}BC} = \varphi_{i+1}{r_{i+1}}^2 = {r_{i+1}}^2 cos^{-1}\frac{r_i sin\theta_i - d}{r_{i+1}} \tag{23}$$

$$S_{\Delta A_iBC} = |A_iD| * |CD| = \frac{1}{2}{r_i}^2 sin2\theta_i \tag{24}$$

$$S_{\Delta A_{i+1}BC} = |A_{i+1}D| * |CD| = (r_i sin\theta_i - d) r_i cos\theta_i \tag{25}$$

The nonoverlapping area of the circle centered at A_{i+1} with that centered at A_i respectively, is given by,

$$S_{A_{i+1}-(A_i \cap A_{i+1})} = \left(S_{\nabla A_{i+1}BC} - S_{\Delta A_{i+1}BC}\right) - \left(S_{\nabla A_i BC} - S_{\Delta A_i BC}\right) \quad (26)$$

Substituting in the above from (22-25), then,

$$S_{A_{i+1}-(A_i \cap A_{i+1})} = \left\{{r_{i+1}}^2 cos^{-1}\frac{r_i sin\theta_i - d}{r_{i+1}} - (r_i sin\theta_i - d) r_i cos\theta_i\right\} - \left\{{r_{i+1}}^2\left(\frac{\pi}{2} - \theta_i\right) - \frac{1}{2}{r_i}^2 sin2\theta_i\right\} \quad (27)$$

As may be seen the expression for the nonoverlapping area differs from the previous case given in (16). Substituting (27) into (3) gives the conditional probability of no handover for this case,

$$P_r(no\ handover\ |r_i\ and\ \theta_i) = \exp\left\{-\lambda\left[\left[{r_{i+1}}^2 cos^{-1}\frac{r_i sin\theta_i - d}{r_{i+1}} - (r_i sin\theta_i - d) r_i cos\theta_i\right] - \left[{r_{i+1}}^2\left(\frac{\pi}{2} - \theta_{i+1}\right) - \frac{1}{2}{r_i}^2 sin2\theta_i\right]\right]\right\} \quad (28)$$

Case (iii) : Tagged base station C is in quadrant *IV*.

This case is shown in Fig. 8, again derivation of the probability of no handover is similar to the previous cases, therefore, we will only explain the differences and otherwise present the results.
For convenience in this analysis θ_i will be measured counterclockwise from the horizontal axis.

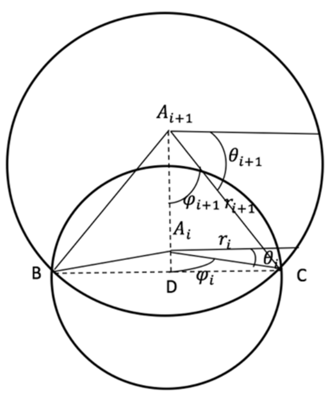

Figure 8: The network diagram when tagged base station *C* is in quadrant *IV*.

From Fig. 8, we let D denote the extension of the line $A_i A_{i+1}$ that intersects with BC. Then, we have,

$$|A_i D| = r_i sin\theta_i, \qquad |A_{i+1} D| = r_i sin\theta_i + d,$$

$$|CD| = |BD| = r_i cos\theta_i \quad (29)$$

As may be seen, $|A_{i+1}D|$ differs from the previous cases. Next, we give the equations corresponding to (6-12) for this case,

$$r_{i+1} = \sqrt{(r_i sin\theta_i + d)^2 + {r_i}^2 cos^2\theta_i} \quad (30)$$

$$\varphi_{i+1} = cos^{-1}\frac{|A_{i+1}D|}{|A_{i+1}C|} = cos^{-1}\frac{r_i sin\theta_i + d}{r_{i+1}} \quad (31)$$

$$\theta_{i+1} = \frac{\pi}{2} - cos^{-1}\frac{r_i sin\theta_i + d}{r_{i+1}} \quad (32)$$

$$\varphi_i = \frac{\pi}{2} - \theta_i \quad (33)$$

$$S_{\nabla A_i BC} = \varphi_i {r_i}^2 = {r_i}^2\left(\frac{\pi}{2} - \theta_i\right) \quad (34)$$

$$S_{\nabla A_{i+1}BC} = \varphi_{i+1}{r_{i+1}}^2 = {r_{i+1}}^2 cos^{-1}\frac{r_i sin\theta_i + d}{r_{i+1}} \quad (35)$$

$$S_{\Delta A_i BC} = |A_i D| * |CD| = \frac{1}{2}{r_i}^2 sin2\theta_i \quad (36)$$

$$S_{\Delta A_{i+1}BC} = |A_{i+1}D| * |CD| = (r_i sin\theta_i + d) r_i cos\theta_i \quad (37)$$

Then, the area of the intersection of the circles centered at A_i and A_{i+1} respectively, is given by,

$$S_{A_i \cap A_{i+1}} = S_{A_i} - \left[\left(S_{\nabla A_{i+1}BC} - S_{\Delta A_{i+1}BC}\right) - \left(S_{\nabla A_i BC} - S_{\Delta A_i BC}\right)\right] \quad (38)$$

where S_{A_i} is given by,

$$S_{A_i} = \pi r_i^2 \quad (39)$$

Substituting in (38) from (34 -37) and (39), then,

$$S_{A_i \cap A_{i+1}} = \pi r_i^2 - \left[\left\{{r_{i+1}}^2 cos^{-1}\frac{r_i sin\theta_i + d}{r_{i+1}} - (r_i sin\theta_i + d) r_i cos\theta_i\right\} - \left\{{r_{i+1}}^2\left(\frac{\pi}{2} - \theta_i\right) - \frac{1}{2}{r_i}^2 sin2\theta_i\right\}\right] \quad (40)$$

Next, the area of the circle at A_{i+1} that does not overlap with circle A_i ,

$$S_{A_{i+1}-(A_i \cap A_{i+1})} = S_{A_{i+1}} - S_{A_i \cap A_{i+1}} \quad (41)$$

where $S_{A_{i+1}}$ is area of the circle A_{i+1} given by,

$$S_{A_{i+1}} = \pi r_{i+1}^2 \quad (42)$$

Next, substituting (40, 42) in (41) and then the result in (3) gives,

$$P_r(no\ handover\ |r_i\ and\ \theta_i) = \exp\left[-\lambda\left\{\pi {r_{i+1}}^2 - \left[\pi r_i^2 - \left[\left\{{r_{i+1}}^2 cos^{-1}\frac{r_i sin\theta_i + d}{r_{i+1}} - (r_i sin\theta_i + d) r_i cos\theta_i\right\} - \left\{{r_{i+1}}^2\left(\frac{\pi}{2} - \theta_i\right) - \frac{1}{2}{r_i}^2 sin2\theta_i\right\}\right]\right]\right\}\right] \quad (43)$$

4 DETERMINING PROBABILITY DISTRIBUTION OF PATH LENGTH WITHOUT HANDOVER

Next, we will determine probability distribution of path length without handover. Let us assume that when the user is at position A_1, it is being served by the base station *C*. From the results of the previous section, probability of no handover may be determined recursively as the user moves from one position to the next one.

If path length without handover is ℓ or more steps it means that when the user is at location A_ℓ it is still being served by station *C*.

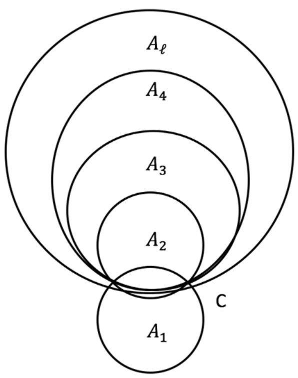

Figure 9: The network diagram as the user moves from position A_1 towards A_ℓ with the initial tagged base station being *C*.

Let us define,

$F_\ell = P_r(\text{no handover is at least } \ell \text{ steps}),\ \ell \geq 1.$

$P_\ell = P_r(\text{no handover is } \ell \text{ steps}),\ \ell \geq 0.$

Next, we will determine these probabilities conditioned on the location of the base station *C*, r_1, θ_1.

Defining,

$F_{\ell|r_1,\theta_1} = P_r(\text{no handover is at least } \ell \text{ steps} \mid r_1, \theta_1)$

$P_{\ell|r_1,\theta_1} = P_r(\text{no handover is } \ell \text{ steps} \mid r_1, \theta_1)$

Then, we have,

$$F_{\ell|r_1,\theta_1} = \prod_{i=2}^{\ell+1} P_r(no\ stations\ in\ S_{A_i-(A_{i-1}\cap A_i)} \mid r_1 and\ \theta_1),\quad \ell \geq 1 \tag{44}$$

$$P_{\ell|r_1,\theta_1} = F_{\ell|r_1,\theta_1} - F_{\ell+1|r_1,\theta_1},\ \ell \geq 1 \tag{45}$$

$$P_{\ell|r_1,\theta_1} = 1 - P_r\big(no\ base\ station\ in\ S_{A_2-(A_1\cap A_2)} | r_1 and\ \theta_1\big),\quad \ell = 0.$$

Finally, unconditional distribution of probability that path length with no handover equals to ℓ steps is given by,

$$P_\ell = \int_0^{2\pi}\int_0^{\infty} P_{\ell|r_1,\theta_1} f(r_1,\theta_1) dr_1 d\theta_1 \tag{46}$$

where $f(r_1,\theta_1)$ is the joint probability density function (pdf) of the location of the tagged base station when the user is at location A_1, next we will determine this joint pdf. Let us define the following probability distribution,

$G(r_1) = P_r(\text{when the user is at location } A_1 \text{ and its distance to station } C \text{ is less than } r_1)$

$G(r_1) = 1 - P_r(\text{no base station within the circle centered at } A_1 \text{ and radius } r_1)$

From equation (1),

$$G(r_1) = 1 - e^{-\lambda\pi r_1^2} \tag{47}$$

Then, pdf of the user distance when it's at $A_1$to the tagged base station is given by,

$$g(r_1) = \frac{dG(r_1)}{dr_1} = 2\lambda\pi r_1 e^{-\lambda\pi r_1^2},\ r_1 > 0. \tag{48}$$

Since the tagged base station is equally likely to be at any location on the circle centered at A_1 with radius of r_1, the pdf of θ_1 is given by,

$$h(\theta_1) = \frac{1}{2\pi},\qquad 0 < \theta_1 < 2\pi \tag{49}$$

and joint pdf is given by,

$$f(r_1,\theta_1) = g(r_1)h(\theta_1) \tag{50}$$

We note that the double integral in (46) does not have a closed form and it needs to be evaluated numerically.

The average path length without hand over is given by,

$$\bar{L} = \sum_{\ell=1}^{\infty} \ell P_\ell \tag{51}$$

5 NUMERICAL RESULTS

In this section, we present numerical results regarding the analysis in the paper as well as simulation results for comparison. The results are given for three cell sizes with radiuses, 50, 100 and 200m. We assume that the step size is $d = 1m$, We note that step size may be chosen arbitrarily small to achieve any accuracy.

Table 1. shows the average path length without handover for both analysis and simulation. As may be seen, the numerical and simulation results are very close to each other. It's also seen that the average path length without handover increases with increasing cell radius. Figures 10-15 show the probability of path

length without handover as a function of the number of steps for both analysis and simulation for the three cell sizes. It may be seen that probability of no handover drops down gradually with increasing path length. As may be seen again, analysis and simulation results are in agreement with each other, which gives further evidence that the analysis is correct.

r(m)	Analysis	Simulation
50	40.76	40.62
100	82.01	82.53
200	164.50	165.02

Table. 1: Average path length without handover for both analysis and simulation for cell sizes with radiuses 50, 100 and 200m.

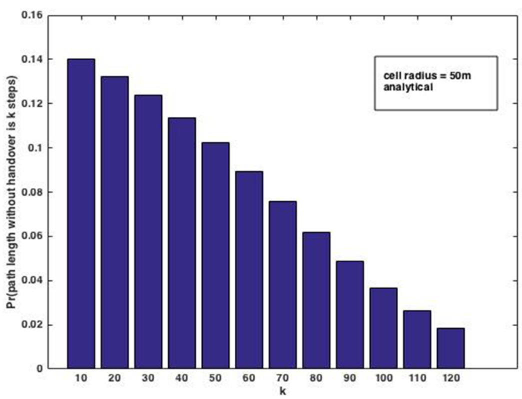

Figure 10: Probability of path length without handover for cell radius of 50m from analysiss.

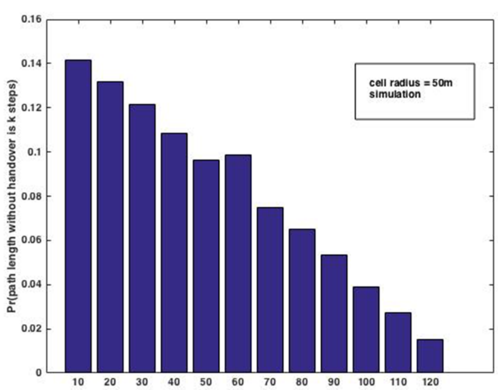

Figure 11: Probability of path length without handover for cell radius of 50m from simulation.

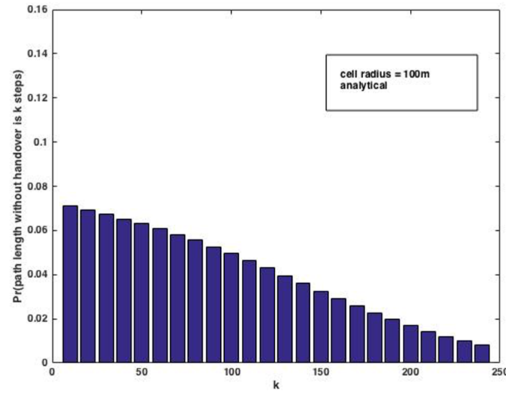

Figure 12: Probability of path length without handover for cell radius of 100m from analysis.

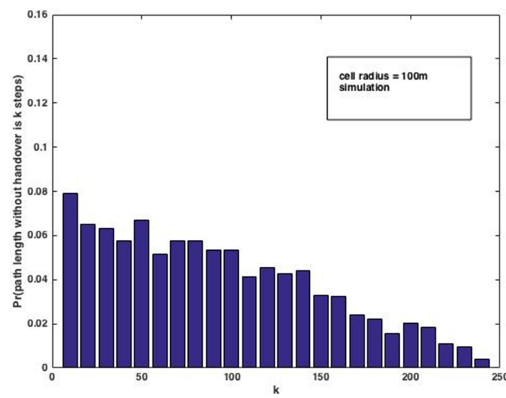

Figure 13: Probability of path length without handover for cell radius of 100m from simulation.

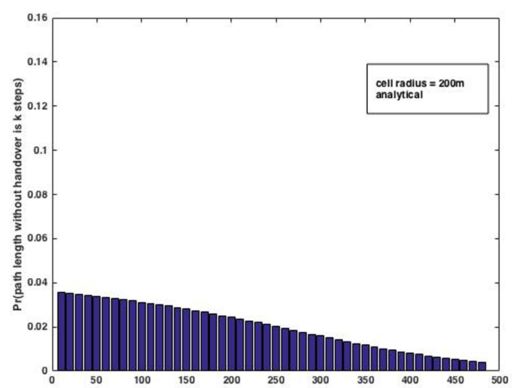

Figure 14: Probability of path length without handover for cell radius of 200m from analysis.

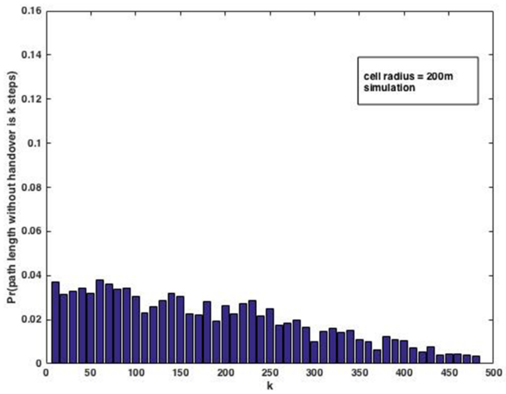

Figure 15: Probability of path length without handover for cell radius of 200m from simulation.

6 CONCLUSIONS

In this paper, we have studied user mobility in cellular networks. We have derived probability distribution of path length without handover as the user moves along a straight line. The analytical and simulation results are in agreement with each other which provides further proof that analysis is correct. To the best of our knowledge, this is the first result on the path length distribution of the user with the same base station. The knowledge of the probability distribution of path length without handover will enable better assessment of the impact of handover on the performance of the system.

REFERENCES

[1] B. U. Kazi and G. Wainer, "Handover enhancement for LTE- advanced and beyond heterogeneous cellular networks", Proceedings of International Symposium on Performance Evaluation of Computer and Telecommunication Systems (SPECTS), pp. 1-8, 2017.

[2] F. Ashtiani, J. Salehi, and M. Aref, "Mobility modeling and analytical solution for spatial traffic distribution in wireless multimedia networks', IEEE Journal on Selected Areas on Communications, Vol.21, No: 10, pp. 1699-1709, Dec. 2003.

[3] Y. Chen, J. Kurose, and D. Towsley, "A mixed queueing network model of mobility in a campus wireless network", Proceedings of IEEE INFOCOM, pp. 2656-2660, March 2012.

[4] J. G. Andrews, F. Baccelli, and R. K. Ganti, "A tractable approach to coverage and rate in cellular networks", IEEE Transactions on Communications, Vol. 59, No. 11, pp. 3122-3134, 2011.

[5] X. Lin, R. K. Ganti, P. J. Fleming and J. G. Andrews, "Towards understanding the fundamentals of mobility in cellular networks", IEEE Transactions on Wireless Communications, Vol. 12, No. 4, pp. 1686-1698, 2013.

[6] W. Bao and B. Liang, "Stochastic geometry analysis of user mobility in heterogeneous wireless networks", IEEE Journal on Selected Areas in Communications, Vol. 33, No. 10, pp. 2212-2225, 2015.

[7] H. Sato, "Theoretical Analysis of Handover and Dynamic Cell Reconfiguration Through Monitored Vehicular Speed", Proceedings of the IEEE International Symposium on Personal, Indoor and Mobile Radio Communications (PIMRC), Montreal.